Power Quality Improvement of Distribution Network Using BESS and Capacitor Bank

F. R. Islam, A. Lallu, K. A. Mamun, K. Prakash, and N. K. Roy

Abstract—**The power demand around the world is increasing rapidly. The aging distribution network architectures are used by the existing utility companies to deliver power to the consumers, which significantly affects the reliability, stability and quality of the delivered power. Different techniques such as compensation devices have been used by power system engineers and researchers to maintain the quality of power transmitted to end users. In this paper, wattage and volt-amp reactive (VAR) planning scheme has been proposed by using the combination of battery energy storage systems and compensators to deal with the vulnerability of networks to voltage drop and system inefficiency. The cost-effective combination of battery energy storage system (BESS) and shunt capacitor bank will then be analyzed to indicate the benefit of the proposed scheme.**

Index Terms—**Battery energy storage system (BESS), shunt capacitor bank, reliability, stability, quality, volt-amp reactive (VAR) planning, distribution network.**

I. Introduction

ELECTRICAL utility companies around the world are under enormous societal and political pressure while designing more efficient electric power grids that implement strategies to reduce energy losses. One of the strategies is to reduce the amount of reactive power supplied to the loads through transmission and distribution lines. In others words, the higher the reactive power demand, the less efficient the grids become for the utilities.

In recent years, volt-amp reactive (VAR) compensators such as static synchronous compensator (STATCOM) and series/shunt capacitors have been used to compensate power on the grid. These compensators provide faster time response and are quite useful as they inject and/or absorb active and reactive power simultaneously to support loads rather than overload the main lines. The implementation of such devices helps increase the apparent power through transmission lines and improves the stability in the network by allowing adjustment of parameters, i. e., frequency, voltage, current, phase angle and impedance.

Placing compensators at the reactive load center can eliminate the reactive load of distribution systems, and the reactive power delivered from the generator will be reduced. The real power loads will be served if the generator is available at full capacity [1]. The reactive load that lags current demand can be effectively eliminated by the leading current which can be provided by the capacitors. The compensator will be able to provide support for the reactive load and voltage improvement, while the performance of the compensator will depend upon the location of the load center [2]. In addition, the harmonic distortion reduces the efficiency of the energy transfer or power factor (PF) [3], [4].

In distribution systems, the structure and configuration of networks can differ significantly depending on the type of loads that define whether the electric power supplied to the end user will be medium or low voltage (LV). For instance, in rural areas, the overhead lines with short interconnection configuration are used, whereas in the urban areas, many lateral connections are used for alternative route of supplies [5]. In this paper, a VAR planning scheme will be carried out by power flow analysis to determine the optimal placement of battery energy storage system (BESS) and capacitor in four different distribution networks, i.e., radial, ring, mesh and aromatic [5], using Electrical Transient and Analysis Program (ETAP) software.

II. Economic Analysis of VAR Planning

Several factors can affect the active and reactive energy prices. Therefore, accurate cost-based pricing is highly difficult, and there is a lack of appropriate exact payment examples internationally. The following chargeable indicators can be used to categorize the applied reactive energy payment techniques around the world: ① peak demand of apparent power; ② apparent energy consumption in kVAh; ③ peak demand in active and reactive power; ④ energy consumption and PF; ⑤ adjusting active power or active energy bills.

Several researches have been conducted and discussions have been made to optimize the capacity of distributed generation (DG) [6]. For instance, genetic algorithm (GA) based optimization model for a standalone photovoltaic (PV)-wind hybrid system including PV battery chargers has been developed in [7], [8]. For larger-scale isolated and grid-connected wind-solar-storage hybrid systems, the optimal DG size and BESS capacity have been addressed in [9]. In [10], the opti-

Manuscript received: May 7, 2019; accepted: November 26, 2019. Date of CrossCheck: November 26, 2019. Date of online publication: XX XX, XXXX.

F. R. Islam (corresponding author) is with University of Sunshine Coast, Sippy Downs, Australia (e-mail: fislam@usc.edu.au).

A. Lallu, K. A. Mamun and K. Prakash are with University of South Pacific, Suva, Fiji (e-mail: avneellallu@gmail.com; kabir.mamun@usp.ac.fj; krishneel.prakash @usp.ac.fj).

N. K. Roy is with Khulna University of Engineering and Technology, Khulna, Bangladesh (e-mail: naruttam.roy@ghd.com).

DOI: 10.35833/MPCE.2019.000304

mal placement of BESS is evaluated using GA for minimizing net present values related to power losses to determine the best operation cost. The STATCOM BESS is studied for nonlinear load and hysteresis controller for the grid operation in [11]. Reference [12] discusses the uses of ultra-capacitor and BESS with shunt capacitor that has been recently used as auxiliary devices for large-scale PV generator system. In [13], BESS and capacitor are discussed and supported by dynamic voltage restorer (DVR) integrated with ultra-capacitor-based rechargeable energy storage to improve its voltage restoration capabilities. In [14], the cost, system losses and installation of larger battery capacity with shunt capacitor are highlighted.

This research will highlight and compare the existing and patent network structure called aromatic network [5]. The IEEE 13-bus network has been modified to form the radial, ring and mesh networks. The single-line diagram for radial, ring and mesh networks is shown in Fig. 1 and distinguished in Table I. The aromatic network is shown in Fig. 2.

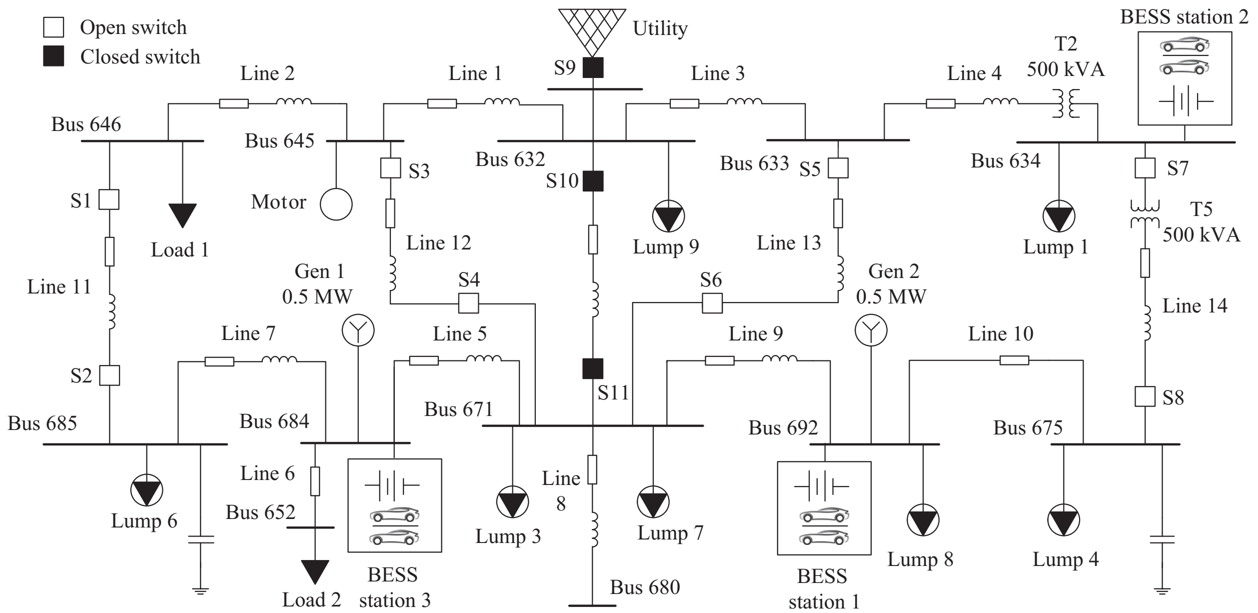

Fig. 1. Single-line diagram of IEEE 13-bus network connected to radial, ring and mesh networks.

TABLE I
SWITCHES FOR IEEE 13-BUS NETWORK

Network	Switch status										
	S1	S2	S3	S4	S5	S6	S7	S8	S9	S10	S11
Radial	Open	Open	Open	Open	Open	Open	Open	Open	Closed	Closed	Closed
Ring	Closed	Closed	Open	Open	Open	Open	Closed	Closed	Closed	Open	Open
Mesh	Closed	Closed	Closed	Closed	Closed	Closed	Closed	Closed	Closed	Open	Open

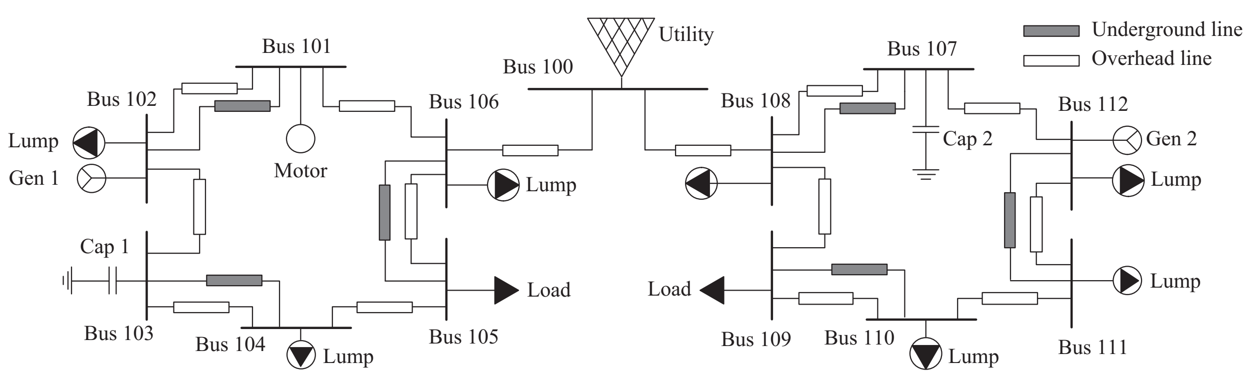

Fig. 2. Dichloro-diphenyl-trichloroethane (DDT) structured aromatic network.

A. Radial Network Architecture

The most common type of distribution network for power distribution system is radial network, which uses only one path between each customer and the substation. The radial network topology has a tree-shape structure, where closed loop does not exist. Therefore, the power can be delivered from one bus to another without tracking down the original bus. However, the power flow need find the original bus while turning backwards [1], [15].

B. Ring Network Architecture

An alternative to the design of a purely radial feeder is the ring network, which has two paths between the power sources (substations and service transformers) [16]. The equipment is sized so that the service can be maintained with a single fault. Concerning the complexity of this network, a loop feeder system is slightly more complex than a radial network [17].

C. Mesh Network Architecture

A mesh network follows the radial structure, but includes redundant distribution lines in addition to the main lines to act as the backup routes during failures or faults. In a mesh network, a wide range of power transfer paths are available, which guarantees significant flexibility in the event of required maintenance or a fault on part of the system [15].

D. Aromatic Network Architecture

Recently, a novel smart distribution network, i.e., aromatic network, has been developed [5], [18]. The design of this network follows the structure of aromatic molecule DDT that comprises of two benzene networks connecting each other through the slack bus as shown in Fig. 2. Each benzene network has six nodes and each node has connections of single and double bonded wiring. The single bond represents the overhead lines, whereas the double bonds represent the combination of overhead and underground wiring. The single and double bonded wiring of the aromatic network provides self-healing characteristics.

III. PF Problems

In rural power distribution systems, the PF usually drops as the demand increases. With an increase in the load and decrease in the PF, the following problems may arise [1], [16]: ① voltage fluctuation; ② the increase of system losses; ③ PF penalties to the customers for high reactive power usage; ④ the reduction of system capacity.

PF is defined as the ratio between real power (W) and total power (VA). To improve the system PF, battery storage systems and capacitors can also offer voltage drop correction with leading current of capacitor. The large amount of inductive VAR current requires bulk power facilities carried to the distribution system, which leads to losses on the bulk facilities and introduces unnecessary cost.

IV. Capacitor Sizing and Placement for Loss Reduction

The optimal placement of capacitor is generally a hard-combinatorial optimization problem that can be formulated as a nonlinear multi-objective problem. A method to reduce the probability of overload in local distribution power network has been achieved by offsetting the electricity transmission congestion and employing local energy storage item in fast power charging station [19]. According to [20], in ETAP, the optimal location of capacitors is defined using the loss sensitivity factor (LSF). The real power loss P_{loss} in the network of branch m is given by:

$$P_{loss}=\frac{r_m\left(P_m^2+Q_m^2\right)}{V_m^2} \tag{1}$$

where r_m is the resistance in branch m; V_m is the voltage profile of bus m; and P_m and Q_m are the real and reactive power drawn from bus m, respectively.

The LSF of the network branches and the net system loss of the real power TP_{loss} in the network can be identified using:

$$LSF=\frac{\partial P_{loss}}{\partial Q_{loss}}=\frac{2Q_m r_m}{V_m^2} \tag{2}$$

$$W_m=\frac{r_m}{V_m^2} \tag{3}$$

$$TP_{loss}=\sum_{m=1}^{N}W_m\left(P_m^2+Q_m^2\right) \tag{4}$$

where N is the number of branches; Q_{loss} is the reactive power loss; and W_m is the the complex magnitude of branch m.

The net real power loss TP_{loss}^{cap} after the optimal installation of capacitors in the network is given by:

$$\begin{aligned}TP_{loss}^{cap}=&\sum_{m\in B_{cap}}W_m\left[P_m^2+\left(Q_m^2-\sum_{k=1}^{z}B_{mk}Q_k^{cap}\right)\right]+\\&\sum_{m\notin B_{cap}}W_m\left(P_m^2+Q_m^2\right)\end{aligned} \tag{5}$$

$$B_{mk}=\begin{cases}1 & Q_k^c \text{ at } k^{\text{th}} \text{ node flows through } m\\ 0 & \text{otherwise}\end{cases} \tag{6}$$

where $m\in B_{cap}$ depicts that branch m is for B_{cap}; B_{cap} is the capacitor bank branch; Q_k^{cap} is the reactive power of bus k; z is the number of capacitors; B_{mk} is the element of a binary matrix $\boldsymbol{B}_{mk}$ with dimension of $B_{cap}\times z$; and Q_k^C is the reactive power of capacitor at branch k.

$\boldsymbol{B}_{mk}$ represents a binary matrix ($B_{cap}\times z$) whose elements can be deduced as:

The net real power loss saved after optimal installation of capacitors $Q_{k,\,opt}^{cap}$ in the network is given by:

$$\begin{aligned}&\Delta TP_{loss}=TP_{loss}-TP_{loss}^{cap}=\\&\sum_{m\in B_{cap}}W_m\left[2Q_m\sum_{k=1}^{z}B_{mk}Q_k^{cap}-\left(\sum_{k=1}^{z}B_{mk}Q_k^{cap}\right)^2\right]\end{aligned} \tag{7}$$

Differentiating (7) with respect to Q_i^{cap} at bus i will give the maximum real power loss as:

$$\frac{\partial\Delta TP_{loss}}{\partial Q_i^{cap}}=2\sum_{m\in B_{cap}}\left[B_mW_m-\left(Q_m-\sum_{k=1}^{z}B_{mk}Q_k^{cap}\right)\right]\quad i\in z \tag{8}$$

The net maximum real power loss saved at the first differentiation equals zero:

$$\left.\frac{\partial\Delta TP_{loss}}{\partial Q_i^{cap}}\right|_{Q_k^{cap}=Q_{k,\,opt}^{cap}}=0=\sum_{m\in B_{cap}}B_{mi}W_m\sum_{k=1}^{z}B_{mk}Q_{k,\,opt}^{cap}=\sum_{m\in B_{cap}}B_mW_mQ_m \tag{9}$$

A matrix representation of the sizes of capacitors at multiple locations in a network is given in (10), or in an expanded form in (11):

$$[Q_{opt}^{cap}]_{Z\times 1}=[X]_{Z\times Z}^{-1}[Y]_{Z\times 1} \tag{10}$$

$$\begin{bmatrix} Q_{1,opt}^{cap} \\ Q_{2,opt}^{cap} \\ \vdots \\ Q_{Z,opt}^{cap} \end{bmatrix}=\begin{bmatrix} X_{1,1} & X_{1,2} & \cdots & X_{1,Z} \\ X_{2,1} & X_{2,2} & \cdots & X_{2,Z} \\ \vdots & \vdots & & \vdots \\ X_{Z,1} & X_{Z,2} & \cdots & X_{Z,Z} \end{bmatrix}\begin{bmatrix} Y_1 \\ Y_2 \\ \vdots \\ Y_Z \end{bmatrix} \tag{11}$$

where Z is a positive integer. The elements of $\boldsymbol{X}$ and $\boldsymbol{Y}$ in (10) are calculated as: $X_h=\sum_{m\in B_{cap}} B_{mg}W_mQ_{mh}$, $Y_h=\sum_{m\in B_{cap}} B_{mh}W_mQ_m$, where B_{mg} (or B_{mh}) is set to 1 if Q_g^c (or Q_h^c) at the g^{th} (or h^{th}) node flows through m; otherwise, it is set to 0. Q_g^c and Q_h^c are the reactive power of capacitor at branch g and h, respectively.

Hence, by using this LSF method, the amount of capacitor bank has been distributed over each network based on the amount of real and reactive losses. The capacitor sizing can be done using:

$$Q_c=V_mI_c \tag{12}$$

where Q_c is the capacitor size; V_m is the voltage magnitude of bus m; and I_c is the capacitor current.

Based on a given set of battery characteristic curves available in the ETAP library, the required battery size for the specified duty cycle can be determined using:

$$W_h=\frac{WHT}{7} \tag{13}$$

$$A_h=\frac{W_h}{0.8V} \tag{14}$$

where W_h is the total energy required; W is the total load; H is the hours of usage; T is the number of days; A_h is the battery capacity; and V is the system voltage.

V. Optimum Placement of BESS and Capacitor

The battery size has been determined for low-level penetration of battery energy storage supply for three different buses, which are considered as charging stations or BESS near heavily loaded nodes around the distribution networks. Each DC station can supply 1%, 2% and 3% of the total capacity of the networks, respectively.

The BESS stations are installed near high-dense distributed loads. The battery capacity should satisfy the minimum voltage requirements to supply DC loads and be converted to AC power. The requirements include: ① the charging voltage applied to the battery should not be more than the maximum system voltage; ② the discharging battery voltage should not be less than the minimum system voltage.

The permanent locations of capacitors should be 1/2 to 2/3 of the total length of the line from the substation (considering "rule of thumb") to obtain the maximum benefits of quality improvement and loss reduction due to uniformly distributed loads. The main constraints for the placement of capacitor have been explained in Fig. 3 [21]. The constraints are as follows: ① the PF should be greater than a threshold; ② all voltage magnitudes of load (PQ) buses should be within the lower and upper bars; ③ the minimum PF bar is met. To place BESS and capacitor banks in power systems, the following should be taken into consideration: ① bank size; ② the location for connection; ③ the connection type of the transformer (Y or Δ).

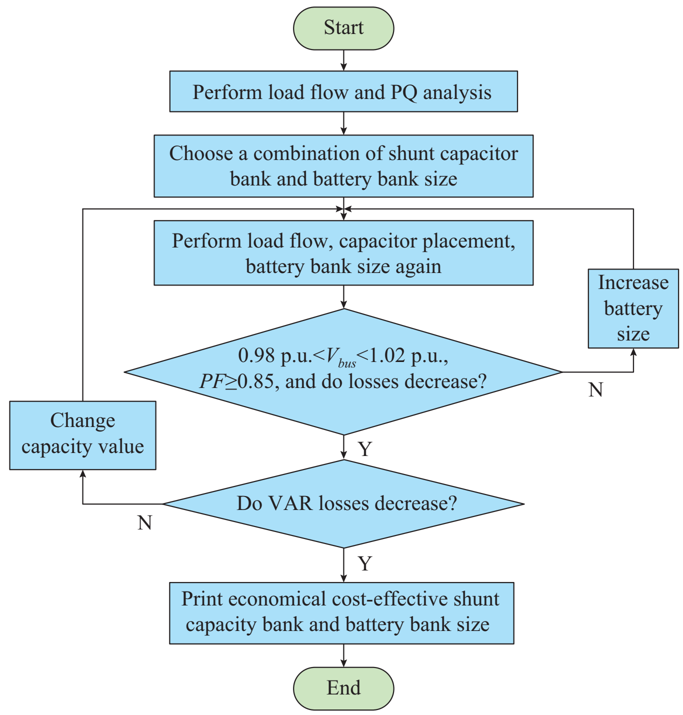

Fig. 3. VAR planning scheme for optimal placement of compensators.

Tables II and III present the load data of the aforementioned distribution networks. The bus numbers identified with asterisk * have PFs which are unreliable or within unstable limits.

The objective of optimal placement of battery storage and capacitor is to minimize the cost of the system. The cost includes five parts for 10-year period that are listed as fol-

TABLE II
IEEE 13-Bus Load Data for Radial, Ring and Mesh Networks

Bus No.	Bus ID	Active power (kW)	Reactive power (kvar)	PF
1				
2	632	100	50	87
3	645	183	79	92
4	646	230	132	87
5	633			
6	634*	400	290	81
7	671	1254	317	97
8	684			
9	652*	128	86	83
10	685	170	80	90
11	680			
12	692*	170	151	75
13	675	843	462	88
Total		3478	1647	

lows: ① the energy cost of electric vehicle (EV) Li-ion battery is 150 $/kWh; ② the installation cost of capacitor is $3000; ③ the purchase cost of capacitor is 350 $/kvar; ④ the operation (maintenance and depreciation) cost of capacitor bank is 300 $ per bank year; ⑤ the cost of real power losses is 0.16 $/kWh.

The flowchart highlights the two types of constraints which have been considered for the lower and upper percentage limits in the following area: ① voltage range (98%-102%, the expected value is 100%); ② PF range (more than 0.83 lagging, the expected value is 0.85 lagging).

TABLE III
LOAD DATA FOR AROMATIC BUS NETWORKS

Bus No.	Bus ID	Active power (kW)	Reactive power (kvar)	PF
1	100	-	-	-
2	106*	170	151	75
3	101	183	79	92
4	102	170	80	90
5	103	-	-	-
6	104	100	58	87
7	105*	128	86	83
8	108	100	58	87
9	107	-	-	-
10	112	843	462	88
11	111*	400	290	81
12	110	1157	659	87
13	109	230	132	87
Total		3481	2055	

Table IV shows different penetration levels of battery required to support 24 hours for different capacity levels of the grid.

TABLE IV
BATTERY ENERGY STORAGE WITH DIFFERENT PENETRATION LEVELS

Storage capacity (%)	Radial, ring and mesh network (kWh/day)	Aromatic network (kWh/day)
1	834.72	835.44
2	1669.44	1670.88
3	2504.16	2506.32

Considering 1% of the total demand (wattage), i.e., 3478 kW of real power demand, an intermittent supply of 34.78 kWh battery energy storage per hour has been installed for radial, ring and mesh networks. Similarly, for the aromatic network, the real energy storage has been sized to 1% of the total capacity, i.e., 3481 kW of real power demand, and an intermittent supply of battery with capacity of 34.81 kWh per hour has been installed.

Table V demonstrates that the ring network has the highest investment cost. However, over a 10-year analysis, the ring network provides benefits to increase energy efficiency and profit by reducing the loss.

TABLE V
SUMMARY OF ECONOMIC ANALYSIS FOR ALL NETWORK STRUCTURES

Penetration level	Network structure	Minimum voltage (%)	Maximum voltage (%)	Battery and capacitor cost ($/year)	Operation cost ($/year)	Benefit ($/year)
Before battery and capacitor placement	Radial	91.25	98.36	-	-	-
	Ring	86.86	98.09	-	-	-
	Mesh	93.51	98.44	-	-	-
	DDT	91.06	101.35	-	-	-
With 3% battery and 50% capacitor	Radial	99.60	101.15	513312	568835	596366
	Ring	99.42	101.52	1004624	321365	1657150
	Mesh	99.76	101.01	495499	491481	434348
	DDT	99.55	100.00	481187	453433	742566
With 3% battery and 100% capacitor	Radial	99.79	101.39	650999	568835	90536
	Ring	99.58	101.73	1633624	321365	1028150
	Mesh	99.96	101.15	615374	491481	314473
	DDT	99.83	100.52	586749	453433	637003

The Li-ion batteries [22] used in this application are EV batteries with an average cost of 150 $/kWh [23] to power the loads. Three test cases with up to 3% of energy storage penetration into the networks are carried out for the batteries.

VI. SIMULATION RESULTS

From the comparison of the networks, all networks without any compensators have huge line losses, as each line is loaded with constant current load and impedance load. After performing the load flow analysis and optimal placement of capacitor, and applying the VAR planning scheme, the aromatic network has demonstrated an economical benefit/payback period of around 2 years using 50% of the required capacitor demand for the buses, whereas the radial, ring and mesh networks will take 3.5 years to clear up the initial payment into profits.

In addition, the aromatic network is the most resilient network. To deal with losses, this network is efficient and requires less operation cost and the lowest need of compensators. This is demonstrated in Figs. 4 and 5. The ring network has the highest capital investment and will return with the most benefits, generate more profit than other networks in the 10-year period of investment. The comparison of power losses before and after battery placement and capacitor banks for all distribution networks are shown in Table VI.

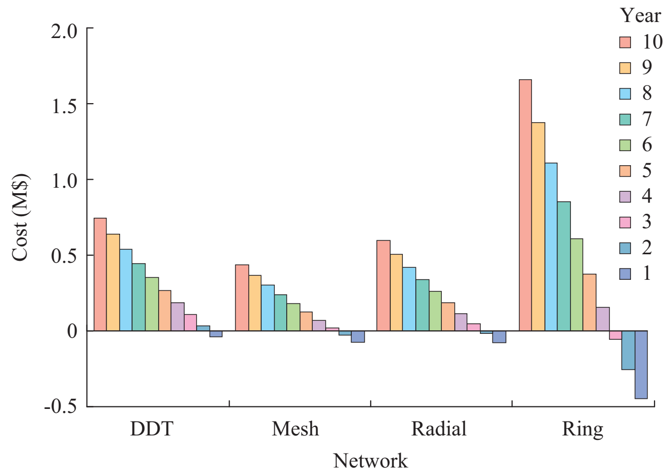

Fig. 4. Accumulative profit in 10 years with 50% capacitor and 3% battery.

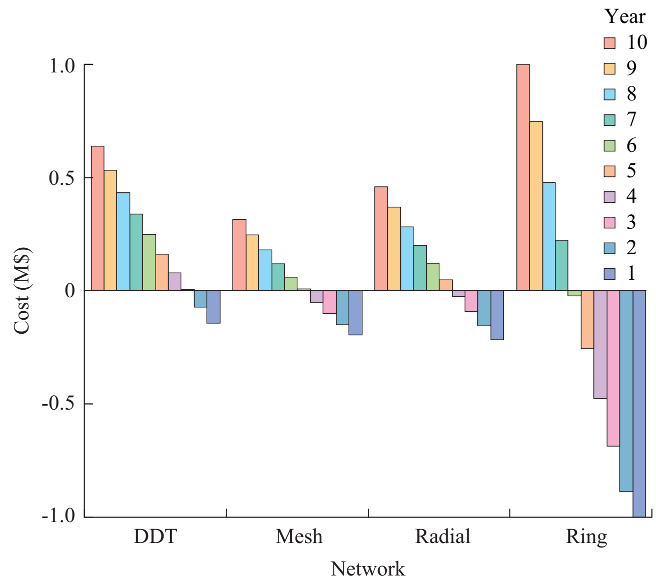

Fig. 5. Accumulative profit in 10 years with 100% capacitor and 3% battery.

Based on the power losses in the system for all four networks using battery energy storage and capacitor banks for penetration of 0%, 1%, 2% and 3% of energy and with 0%, 50% and 100% of reactive power, it can be concluded that an excessive amount of battery and capacitor penetration has less impact to reduce losses, but increases the investment factor, and the system becomes unstable.

The most significant impact of battery penetration is observed with ring network of around 86% in loss reduction in active and reactive power with only 1% battery penetration. However, with 1% implementation of battery energy storage on the mesh network, the system reduces 67% of losses, which is the lowest in the four networks.

The proposed VAR planning scheme reflects how the combination of 50% capacitor and 3% of battery will generate less losses and more benefits in terms of revenue based on the 10-year reliability of the system, which has been summarized and presented in Fig. 6 and Fig. 7, respectively. It is observed that the voltages of the networks increase when the system losses decrease and the power system becomes more reliable. When the load in the lines decreases, the amount of power transmitted to the consumer in each phase has less voltage drop, which causes the voltage to rise towards the desired target.

TABLE VI
ENERGY LOSSES FOR DIFFERENT PENETRATION LEVELS IN RADIAL, RING, MESH AND DDT NETWORKS

Battery (%)	Capacitor (%)	Active power loss (kW)				Reactive power loss (kW)			
		Radial	Ring	Mesh	DDT	Radial	Ring	Mesh	DDT
0	0	159.6	262.6	136.3	119.9	470.7	705.6	404.9	363.1
	50	114.2	174.4	99.8	75.5	337.1	468.8	297.1	228.0
	100	112.5	191.6	97.8	79.4	332.8	517.3	289.3	239.2
1	0	43.0	37.6	44.6	159.5	117.7	100.1	124.0	494.5
	50	36.6	32.5	39.4	115.1	99.4	84.6	108.8	359.3
	100	37.5	38.8	42.1	119.0	100.7	98.4	113.4	370.5
2	0	37.7	34.6	37.9	61.2	103.0	91.3	104.9	194.0
	50	35.1	31.7	35.4	59.7	93.2	81.1	96.2	188.0
	100	36.4	34.5	36.2	61.2	93.8	86.4	96.7	191.5
3	0	34.2	31.2	36.7	61.6	89.7	75.7	96.6	193.7
	50	33.0	30.2	35.6	59.5	83.8	70.6	91.5	187.7
	100	34.1	31.6	36.8	61.6	83.3	70.7	91.7	191.2

VII. CONCLUSION

The dynamic analysis of stability and economic factors using a new planning scheme combination of BESS and capacitor banks in the networks has been proved to be beneficial for the networks. The capacitors compensate VAR power for the excessive reactive loads in the network, while the battery banks assist to deliver real power to the network from different stations, which reduces the load of line.

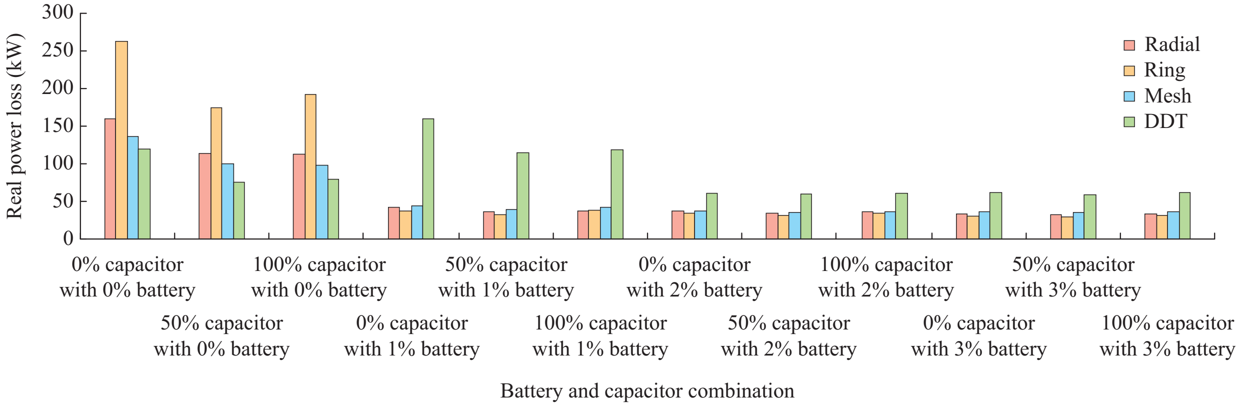

Fig. 6. Active power losses for all networks.

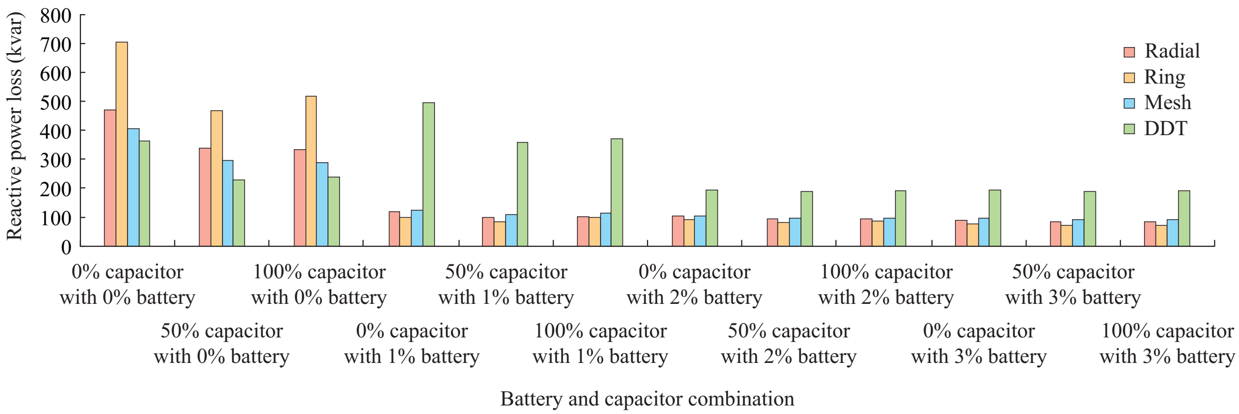

Fig. 7. Reactive power losses for all networks.

The most efficient and cost-effective is the aromatic structure network using 50% capacitor placement and 3% BESS combination. Aromatic network structure demonstrates the quickest benefit/payback period of around 2 years using 50% of the required capacitor demand for the buses, while radial, ring and mesh networks will take 3.5 years to clear up the payback.

As the power networks are expanding around the world, this research work aligns with the engineering solution of adding storage systems to improve the power quality, while considering the reliability of combining different network routing structures with the traditional capacitor bank system.

The research improves the PF, enhanes voltage profile and increases the feeder capacity with less investment and operation cost. The following conclusions can be made:

1) The optimal value of the battery bank will reduce the load of the overhead lines for active power, and capacitor banks will add reactive power to the lines.

2) The algorithm flowchart finds the estimated size and placement of the BESS and capacitor.

3) There is improvement in PF and voltage, which helps increase the feeder capacity.

4) The installation of the battery bank improves PF because of the availability of active and reactive power compensator near the inductive loads.

5) The planting capacitors near demand load centers can be limited.

References

[1] M. Balci and M. Hocaoglu, “Effects of source voltage harmonic distortion on power factor compensation in triac controlled AC chopper circuits,” in *Proceedings of International Conference on Power Electronics and Drives Systems*, Kuala Lumpur, Malaysia, Dec. 2005, pp. 1199-1204.

[2] T. Gonen, *Electrical Power Transmission System Engineering*, 3rd edn. Hoboken, USA: CRC Press, 2015.

[3] A. Anand and B. Singh, “Modified dual output cuk converter-fed switched reluctance motor drive with power factor correction,” *IEEE Transactions on Power Electronics*, vol. 34, no. 1, pp. 624-635, Jan. 2019.

[4] J. Grainger and S. Civanlar, “Volt/var control on distribution systems with lateral branches using switched capacitors and voltage regulators, Part i, Part ii and Part iii,” *IEEE Power Engineering Review*, vol. 5, no. 11, pp. 52-54, 1985.

[5] F. R. Islam, K. Prakash, K. Mamun *et al.*, “Aromatic network: a novel structure for power distribution system,” *IEEE Access*, vol. 5, pp. 25236-25257, Oct 2017.

[6] M. J. Hadidian-Moghaddam, S. Arabi-Nowdeh, and M. Bigdeli, “Optimal sizing of a stand-alone hybrid photovoltaic/wind system using new grey wolf optimizer considering reliability,” *Journal of Renewable and Sustainable Energy*, vol. 8, no.3, pp. 1-10, May 2016.

[7] R. E. Precup, *Solar Photovoltaic Power Plants: Advanced Control and Optimization Techniques*. Berlin: Springer, Feb. 2019.

[8] L. Xu, X. Ruan, C. Mao *et al.*, “An improved optimal sizing method for wind-solar-battery hybrid power system,” *IEEE Transactions on Sustainable Energy*, vol. 4, no. 3, pp. 774-785, Mar. 2013.

[9] J. Eyer and G. Corey, “Energy storage for the electricity grid: benefits and market potential assessment guide,” *Sandia National Laboratories* , vol. 20 , no. 10, pp. 1-5, Feb. 2010.

[10] M. Farsadi, T. Sattarpour, and A. Nejadi, “Optimal placement and operation of BESS in a distribution network considering the net present value of energy losses cost,” in *Proceedings of 9th International Conference on Electrical and Electronics Engineering (ELECO)*, Bursa,

Turkey, Nov. 2015, pp. 434-439.

[11] S. Kirmani and B. Kumar, "Power quality improvement by using STATCOM control scheme in wind energy generation interface to grid," *IOP Conference Series: Earth and Environmental Science*, vol. 114, no.1, pp. 1-10, Jan. 2018.

[12] R. Shah and N. Mithulananthan, "A comparison of ultracapacitor, BESS and shunt capacitor on oscillation damping of power system with large-scale PV plants," in *Proceedings of Universities Power Engineering Conference (AUPEC)*, Brisbane, Australia, Sept. 2011, pp. 1-6.

[13] K. Mounika and C. Sridhar, "Control schemes for improving power quality with BESS and ultra-capacitor supported dynamic voltage restorer," *International Journal of Advance Engineering and Research Development*, vol. 4, no. 4, pp. 1-8, Apr. 2017.

[14] S. Karanki and D. Xu, "Optimal capacity and placement of battery energy storage systems for integrating renewable energy sources in distribution system," in *Proceedings of 2016 National Power Systems Conference (NPSC)*, Bhubaneswar, India, Dec. 2016, pp. 1-6.

[15] K. Prakash, A. Lallu, F. R. Islam et al. "Review of power system distribution network architecture," in *Proceedings of 2016 3rd Asia-Pacific World Congress on Computer Science and Engineering*, Nadi, Fiji, Dec 2016, pp. 1-7.

[16] S. Iwamoto and Y. Tamura, "A load flow calculation method for ill-conditioned power systems," *IEEE Transactions on Power Apparatus and Systems*, vol. 100, no. 4, pp. 1736-1743, Apr. 1981.

[17] Y. Amrane, R. Gueddouche, A. Elmaouhab *et al*., "Optimal capacitor placement and sizing in radial distribution feeders using evolutionary algorithm: a case study of the Algerian-Djanet distribution system," in *Proceedings of International Conference on Electrical Sciences and Technologies in Maghreb (CISTEM)*, Algiers, Algeria, Oct. 2018, pp. 1-6.

[18] F. R. Islam, K. Mamun, K. Prakash *et al*., "Aromatic network for power distribution system," Australia Patent 2 017 100 293, Jan. 2019.

[19] I. Bayram, G. Michailidis, M. Devetsikiotis *et al*., "Local energy storage sizing in plug-in hybrid electric vehicle charging stations under blocking probability constraints," in *Proceedings of 2011 IEEE International Conference on Smart Grid Communications*, Brussels, Belgium, Oct. 2011, pp. 1-6.

[20] Operation Technology, Inc. (2011, May). ETAP user guide. [Online]. Available: https://www. scribd. com/document/219496381/Etap-User-Guide

[21] N. Roy, H. Pota, and M. Hossain, "Reactive power management of distribution networks with wind generation for improving voltage stability," *Renewable Energy*, vol. 58, pp. 85-94, Oct. 2013.

[22] R. Brown, *Electric Power Distribution Reliability*. Boca Raton, USA: CRC Press, 2009.

[23] O. Van Vliet, A. Brouwer, T. Kuramochi *et al*., "Energy use, cost and CO2 emissions of electric cars," *Journal of Power Sources*, vol. 196, no. 4, pp. 2298-2310, Feb. 2011.

F. R. Islam received Ph.D. degree in electrical engineering from the University of New South Wales, Canberra, Australia, in 2013. He is working as a Senior Lecturer of the University of Sun Shine Coast, Sippy Downs, Australia. He was the Publication and Publicity Chair of IEEE Fiji. He is an Associate Editor of IEEE Access. His research interests include microgrid, smart grid, supervisory control and data acquisition (SCADA), electrification of transportation, and control system.

A. Lallu received the B.Eng. and M.Sc.Eng. degrees in electrical and electronics engineering from the University of South Pacific, Suva, Fiji, in 2016 and 2019, respectively. His current research interests include reactive power, distributed generation, energy markets, power supplies, renewable energy sources, and new energy storage devices.

K. A. Mamun received the Ph.D. degree in mechanical and manufacturing engineering from Dublin City University (DCU), Dublin, Ireland, in 2007 and 2012, respectively. He is working as a Senior Lecturer of the University of the South Pacific, Suva, Fiji. His current research interests include renewable and sustainable energy generation.

K. Prakash received the B.Eng. and M.Sc. degrees in electrical and electronic engineering from the University of South Pacific, Suva, Fiji, in 2016 and 2019, respectively. His current interests include reactive power, distributed generation, renewable energy sources, and new energy storage devices.

N. K. Roy received his Ph.D. degree from the University of New South Wales, Canberra, Australia, in 2014. He is an Associate Professor of Khulna University of Engineering and Technology, Khulna, Bangladesh. His current researcher interests include power system stability and renewable energy.